CHEMICAL ENGINEERING TRANSACTIONS Volume 25, 2011
Editors Jiří Jaromír Klemeš, Petar Sabev Varbanov, Hon Loong Lam
 ISBN 978-88-95608-16-7 ISSN 1974-9791
DOI: 10.3303/CET1125118

Kinetics of the Fischer-Tropsch Reaction over a Ru-Promoted Co/Al_2O_3 Catalyst

Tejas Bhatelia[1], Wenping Ma[2], Burtron Davis[2], Gary Jacobs[2] and Dragomir Bukur[1*]

[1]Department of Chemical Engineering, Texas A&M University at Qatar, P O Box 23874, Doha, Qatar
dragomir.bukur@qatar.tamu.edu
[2]Center for Applied Energy Research, University of Kentucky, 2540 Research Park Drive, Lexington, Kentucky, 40511, USA

The kinetics of the Fischer Tropsch (FT) synthesis reaction over 0.27 % Ru 25 % Co/Al_2O_3 catalyst was studied in a 1L stirred tank slurry reactor (STSR). Experiments were conducted at reactor pressures of 1.4 MPa and 2.4 MPa, temperatures of 205 °C and 220°C, H_2/CO feed ratios of 1.4 and 2.1 and gas space velocities ranging from 2 to 15 NL/g-cat·h. Langmuir–Hinshelwood–Hougen–Watson (LHHW) type rate equations were derived on the basis of a set of reactions originating from carbide and enolic pathways for hydrocarbon formation. Derived rate equations were fitted to the corrected experimental rate using Levenberg-Marquardt method to obtain model parameters. Physical and statistical tests were used to discriminate between rival models. It was found that a model based on hydrogen-assisted dissociative adsorption of CO followed by hydrogenation of dissociatively adsorbed CO provides the best fit to the data.

1. Introduction

Depleting oils reserves, environmental pressure, as well as abundant reserves of coal, natural gas and biomass, have all contributed to revive interest in Fischer-Tropsch synthesis (FT) technology. FT technology involves conversion of synthesis gas (i.e., a mixture of H_2 and CO) to hydrocarbons, which can be upgraded by processes such as hydrocracking to produce liquid transportation fuels. FT is a complex reaction that converts synthesis gas to a product distribution consisting of a multi-component mixture of linear and branched hydrocarbons as well as oxygenated products. The reaction is catalyzed by metals or metal carbides of the transition metal elements Co, Fe, and Ru (Dry, 1996). Main products are linear paraffins and α-olefins (Dry, 1996, Schulz, 1999).

2. Theory

Throughout the history of FT and for various cobalt-based catalysts, kinetic studies have been performed by numerous researchers groups. Botes et al. (2009) recently proposed a macro kinetic model over Co catalyst where they found that CO dissociation occurs without hydrogen interaction. Visconti et al. (2010) have also proposed unassisted CO dissociation in their recent work to describe CO conversion and alkyl mechanism for chain growth. However, from quantum chemistry calculations, Ojeda et al. (2010) found

Please cite this article as: Bhatelia T., Ma W., Davis B., Jacobs G. and Bukur D., 2011, Kinetics of the fischer-tropsch reaction over a ru promoted co/al2o3 catalyst, Chemical Engineering Transactions, 25, 707-712
DOI: 10.3303/CET1125118

that this path had high activation energy barrier. Atashi et al. (2010) proposed eleven mechanisms and found that two of their best fitted models were based on hydrogen assisted CO dissociation.
To summarize, proposed rate equations are either in the form of empirical power laws or mechanistic equations of LHHW type (Das et al., 2005). Most of these studies used experimental data obtained over a narrow range of process conditions in integral fixed-bed reactors. Moreover, many of the LHHW rate equations were simplified by neglecting some of the adsorbed species (Sarup and Wojciechowski, 1989). In this study, we have attempted to overcome these shortcomings and have utilized more general LHHW rate equations for the hydrocarbon formation rate. Experiments were conducted over a wide range of operating conditions in the STSR.

2.1 Reaction mechanisms

The LHHW approach was used to derive rate equations. For each model, the possible rate-determining steps were identified and all other steps were assumed to be in quasi-equilibrium. Elementary steps and rate equations for four models considered are summarized in **Errore. L'origine riferimento non è stata trovata.**.

3. Parameter estimation

To estimate parameters, partial pressures for each species –along with the experimental rate (r_{FT}^{exp}) from the experimental database – are required. In total, there were 12 data points at each temperature with CO conversion varying between 8-60 %. One of the most common problems with in any catalytic reaction is the loss of catalyst activity with time, which is due to a variety of deactivation phenomena. To account for catalyst aging, adjustments were made to correct the data to a fresh catalyst basis. To define catalyst aging, a set of reference conditions was returned to at several key points during the kinetic test. Thus, the corrected data were used for parameter estimation. Model parameters were estimated using the Levenberg–Marquardt method by minimizing the following objective function:

$$x^2 = \sum_i \frac{\left(r_{FT}^{exp} - r_{FT}^{mod}\right)^2}{r_{FT}^{exp\,2}} \tag{1}$$

4. Model discrimination

Detailed analysis and model discrimination were performed by applying four models which are based on carbide and enol mechanisms. No a priori assumptions were made with regard to adsorption equilibrium constants of any particular species. Firstly, lumped kinetic constants were estimated, from which pure kinetic constants were extracted and examined for physical and statistical relevance. Sensitivity studies were performed by making assumptions regarding adsorption constants of some species. Optimized models were checked for statistical significance using qualitative (parity curves) and quantitative (R-square, RMSE, F-test) analysis. Finally, for the best-fitted model activation energies and heats of adsorption were calculated.

Table 1: Elementary reactions for FT synthesis

Reaction mechanism	Rate law	k molkg^{-1}s^{-1}MPa^{-n} a,b,m,MPa^{-n}
M_1	$\frac{kP_{CO}^{1/2}P_{H_2}^{1/2}}{\left(1+aP_{CO}^{1/2}+bP_{H_2}^{1/2}+mP_{H_2O}\right)^2}$	$k = (K_{CO1}\, k_{CH}\, K_{CO2}\, K_{H2}\, K_{OH})^{1/2}$
CO+S↔CO–S		$a = (K_{CO2}\, K_{H2}\, k_{OH}/k_{CH})^{1/2}$
H_2+2S↔2H–S		$b = K_{H2}^{1/2}$
CO–S+S↔C–S+O–S		$m = K_{H2O}$
C–S + H–S→CH–S + S		$K_{CO} = K_{CO1} * K_{CO2}$
CH–S+H–S ↔CH_2–S+S		
O–S+H-S→OH–S+ S		
OH–S+H–S↔H_2O-S+S		
H_2O-S↔H_2O+S		
M_2	$\frac{kP_{CO}^{1/2}P_{H_2}}{\left(1+aP_{CO}^{1/2}++mP_{H_2O}\right)}$	$k = (K_{CO1}\, k_{CH2}\, K_{CO2}\, k_{H2O})^{1/2}$
CO+S↔CO–S		$a = (K_{CO1}\, K_{CO2}\, k_{H2O}/k_{CH2})^{1/2}$
CO–S+S↔C–S+O–S		$m = K_{H2O}$
C–S+H_2→CH_2–S		$K_{CO} = K_{CO1} * K_{CO2}$
O–S+H_2 →H_2O-S		
H_2O-S↔H_2O+S		
M_3		$k = k_{HCO}\, K_{CO}\, K_{H2}^{1/2}$
CO+S↔CO–S	$\frac{kP_{CO}P_{H_2}^{1/2}}{\left(1+aP_{CO}+bP_{H_2}^{1/2}+mP_{H_2O}\right)^2}$	$a = K_{CO}$
H_2+2S↔2H–S		$b = K_{H2}^{1/2}$
CO–S+H-S→HCO–S+S		$m = K_{H2O}$
HCO–S+H-S↔C–S+H_2O-S		
C–S+H–S↔CH–S+S		
CH–S+H–S↔CH_2–S+S		
H_2O-S↔H_2O + S		
M_4	$\frac{kP_{CO}P_{H_2}^2}{\left(1+aP_{CO}+bP_{H_2}+mP_{H_2O}\right)}$	$k = K_{CO}\, K_{H2CO}\, k_{CH2}$
CO+S↔CO–S		$a = K_{CO}$
CO–S+H_2↔H_2CO-S		$b = K_{CO}\, K_{H2CO}$
H_2CO-S+H_2→CH_2-S+H_2O-S		$m = K_{H2O}$
H_2O-S↔H_2O+S		
S is active site; K_i and k_i are adsorption and reaction rate constant respectively.		

5. Results and discussion

Table 2 and Table 3 **Errore. L'origine riferimento non è stata trovata.Errore. L'origine riferimento non è stata trovata.**show the values of lumped kinetic constants and intrinsic kinetic constants obtained for all models at both temperatures. In order to avoid negative values for parameters such as adsorption constants, parameters were restricted to realistic ranges during fitting. As shown in Table 3, for model M_1 the kinetic constant k_{CH} increased while the adsorption equilibrium constant for hydrogen decreased with increase in temperature. However, the adsorption equilibrium constant of water increased with temperature, which is unexpected and thus this model was rejected. Similarly, for model M_2 the kinetic constant k_{CH} decreased with the increase in temperature, and this model was also rejected.

For model M_3, the kinetic constant k_{HCO} and the adsorption equilibrium constants for H_2 and CO were found to increase with temperature. This is an unexpected behavior for the adsorption equilibrium constants. Also, it was found that the adsorption constant of water is small at both temperatures. The effect of water on the FT reaction kinetics has been a topic of debate. Botes (2009) recently found that water had no notable influence on the overall rate of CO conversion over Co catalyst. Therefore, new parameter values were estimated assuming that the water does not adsorb strongly on the catalyst surface (Table 4). It can be seen that after removing K_{H20} from the denominator the expected trends for the reaction and adsorption constants were obtained, i.e. the reaction rate constant increased whereas the adsorption constants decreased with increase in temperature.

Table 2: Lumped kinetic constants for all models at both temperatures

	T = 205 °C				T = 220 °C			
	M_1	M_2	M_3	M_4	M_1	M_2	M_3	M_4
k	3.28	75.4	3.6	74.6	3.4	158.5	205	251.5
a	13.94	7.2E3	8.93	200.	9.3	5.8E3	52.3	1.6E3
b	3.39	-	15.1	6.7E3	1.2	-	71.8	7.7E3
m	3.5E-4	1.3E-8	2.2E-14	7.6E-13	1.7	1.E-9	2.2E-14	60.4

Table 3: Kinetic constants extracted from estimated lumped constants

	T = 205 °C				T = 220 °C			
	M_1	M_2	M_3	M_4	M_1	M_2	M_3	M_4
K_{H2}	11.5	-	2.2E2	-	1.4	-	5.1E3	-
K_{H2O}	≈0	≈0	≈0	≈0	1.7	≈0	≈0	6E1
K_{CO}	-	-	8.9	200	-	-	52.3	1.6E3
k_{CH}	0.07	0.2	-	-	0.3	0.02	-	-
$K_{CO}*k_{OH}$	195.1	-	-	-	85.9	-	-	-
$K_{CO}*k_{H2O}$	-	2.8E4	-	-	-	9.3E5	-	-
k_{HCO}	-	-	2.6E2	-	-	-	5.5E2	-
k_{CH2}	-	-	-	0.01	-	-	-	0.03
K_{H2CO}	-	-	-	33.5	-	-	-	4.8

For model M_4 the kinetic constant k_{CH2} increased, whereas adsorption constant K_{H2CO} decreased with increase in temperature. However, adsorption constants of CO and water increased with temperature, which is not the expected behavior. An assumption that water does not inhibit the reaction did not result in improvement. Based on these findings this model was discarded. Thus in summary, from the four models considered, the M_3 model yielded the most physically significant results after optimization, and was further tested for statistical significance.

Apparent activation energy and heats of adsorption were calculated for optimized model M_3. Using Arrhenius dependencies it was found that apparent activation energy for this model was 162 kJ/mol, whereas heats of adsorption for CO and H_2 were 41 and 166 kJ/mol, respectively. Literature values of activation energies, heat of adsorption of CO and H_2 range from 90 to 120 kJ/mol, 70 to 185 kJ/mol and 20 to 105 kJ/mol respectively

(Ribeiro et al., 1997, Zowtiak and Bartholomew, 1983, Vannice, 1975, Yates and Satterfield, 1991). The values of activation energy and heats of adsorptions obtained in the present study, lie outside these ranges. However, values of these parameters depend on the form of LHHW rate expression, metal loading and metal-support interactions.

Table 4: Effect of K_{H2O} on the constants for model M_3

Kinetic constant	$\frac{kP_{CO}P_{H_2}^{1/2}}{\left(1+aP_{CO}+bP_{H_2}^{1/2}+mP_{H_2O}\right)^2}$		$\frac{kP_{CO}P_{H_2}^{1/2}}{\left(1+aP_{CO}+bP_{H_2}^{1/2}\right)^2}$	
	T = 205 °C	T = 220 °C	T = 205 °C	T = 220 °C
k_{HCO}	2.6E-2	5.5E-2	0.08	0.3
K_{CO}	8.9	5.2E1	5.9	4.3
K_{H2}	2.2E2	5.1E3	1.8	0.5
K_{H2O}	≈0	≈0	-	-

5.1 Statistical test

The goodness of fit for model M_3 was checked using several statistical tests (R-square values, root mean square error (RMSE), F-test and parity curves). It was found that RMSE and R-square values were 0.0021 and 0.45, respectively at 205 °C and 0.0115 and 0.49 respectively at 220 °C While the values of R-square appear to be low, they are within the acceptable range since the experimental data do not vary to a statistically significant degree from the average value. This model also passes the critical F-test at both temperatures. Finally, low values of RMSE suggest that model would well predict the experimental reaction rates which is illustrated in **Errore. L'origine riferimento non è stata trovata.**.

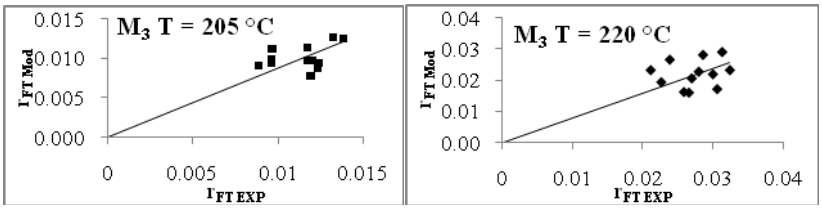

Figure 1: Parity curves for model M_3 at T = 205 °C and T = 220 °C

6. Conclusions

LHHW type rate expressions were derived from carbide and enolic pathways for hydrocarbon formation. Adjustments were made to account for catalyst aging. Model parameters were estimated using the Levenberg–Marquardt method. Rival models were discriminated based on both the physical and statistical significance of estimated parameters. Models M_1 and M_2 did not yield physically meaningful results, whereas model M_3 initially did not fulfill Arrhenius criteria. However, after removing K_{H2O} (i.e., assuming that the water does not adsorb strongly on the catalyst surface) we obtained the expected trends for the reaction and adsorption constants. After the adsorption of

water in the rate law was deleted this model has the same form as one of the two rate laws proposed by Sarup and Wojciechowski, (1989).

When similar assumption was made for the model M_4 it was found that the adsorption constant for CO (K_{CO}) decreased significantly whereas, K_{H2CO} increased by a factor of 13. This, in turn transformed the LHHW rate law to a simple power law. Optimized model M_3, which is based on hydrogen-assisted dissociative adsorption of CO followed by hydrogenation of dissociatively adsorbed CO to form the methylene monomer, resulted in the best and most physically meaningful fitting of the experimental data.

References

Atashi, H., Siami, F., Mirzaei, A. A. and Sarkari, M., 2010, Kinetic study of Fischer-Tropsch process on titania-supported cobalt-manganese catalyst, Journal of Industrial and Engineering Chemistry 16, 952-961.

Botes, F. G., 2009, The influences of water and syngas partial pressure on the kinetics of a commercial alumina-supported cobalt FT catalyst, Industrial and Engineering Chemistry 48, 1859-1865.

Botes, F. G., van Dyk, B. and McGregor, C., 2009, The development of a macro kinetic model for a commercial $Co/Pt/Al_2O_3$ Fischer-Tropsch catalyst, Industrial & Engineering Chemistry Research 48, 10439-10447.

Das, T. K., Conner, W. A., Li, J., Jacobs, G., Dry, M. E. and Davis, B. H., 2005, Fischer-Tropsch Synthesis: Kinetics and Effect of Water for a Co/SiO_2 Catalyst, Energy & Fuels 19, 1430-1439.

Dry, M. E., 1996, Practical and theoretical aspects of the catalytic Fischer-Tropsch process, Applied Catalysis A: General 138, 319-344.

Ojeda, M., Nabar, R., Nilekar, A. U., Ishikawa, A., Mavrikakis, M. and Iglesia, E., 2010, CO activation pathways and the mechanism of Fischer-Tropsch synthesis, Journal of Catalysis 272, 287-297.

Ribeiro, F. H., Wittenau, A. E. S. V., Bartholomew, C. H. and Somorjai, G. A., 1997, Reproducibility of turnover rates in heterogeneous metal catalysis: Compilation of data and guidelines for data analysis, Catalysis Reviews: Science and Engineering 39, 49-76.

Sarup, B. and Wojciechowski, B. W., 1989, Studies of the Fischer-Tropsch synthesis on a cobalt catalyst II. Kinetics of carbon monoxide conversion to methane and to higher hydrocarbons, The Canadian Journal of Chemical Engineering 67, 62-74.

Schulz, H., 1999, Short history and present trends of Fischer-Tropsch synthesis, Applied Catalysis A: General 186, 3-12.

Vannice, M. A., 1975, The catalytic synthesis of hydrocarbons from H_2/CO mixtures over the group VIII metals : II. The kinetics of the methanation reaction over supported metals, Journal of Catalysis 37, 462-473.

Visconti, C. G., Lietti, L., Tronconi, E., Forzatti, P., Zennaro, R. and Rossini, S., 2010, Detailed kinetics of the Fischer-Tropsch synthesis over Co-based catalysts containing sulphur, Catalysis Today 154, 202-209.

Yates, I. C. and Satterfield, C. N., 1991, Intrinsic kinetics of the Fischer-Tropsch synthesis on a cobalt catalyst, Energy & Fuels 5, 168-173.